JOURNAL OF APPLIED PHYSICS **104**, 113722 (2008)

Composition dependence of Schottky barrier heights and bandgap energies of GaN_xAs_{1-x} synthesized by ion implantation and pulsed-laser melting

Taeseok Kim,[1,a)] Kirstin Alberi,[2] Oscar D. Dubon,[3,4] Michael J. Aziz,[1] and Venkatesh Narayanamurti[1]

[1]*Harvard School of Engineering and Applied Sciences, Cambridge, Massachusetts 02138, USA*
[2]*National Renewable Energy Laboratory, Golden, Colorado 80401, USA*
[3]*Department of Materials Science and Engineering, University of California, Berkeley, California 94720, USA*
[4]*Lawrence Berkeley National Laboratory, Berkeley, California 94720, USA*

(Received 30 September 2008; accepted 4 November 2008; published online 11 December 2008)

We present a systematic investigation on the band structure of the GaN_xAs_{1-x} alloys synthesized using nitrogen ion implantation followed by pulsed-laser melting and rapid thermal annealing. The evolution of the nitrogen-concentration depth profile is consistent with liquid-phase diffusion, solute trapping at the rapidly moving solidification front, and surface evaporation. The reduction of the Schottky barrier height of the Γ-like threshold at nitrogen composition up to $x=0.016$ is studied by ballistic electron emission microscopy (BEEM) and determined quantitatively using the second voltage derivative BEEM spectra to be -191 ± 63 meV per $x=0.01$, which is close to the corresponding slope for samples grown by low-temperature molecular beam epitaxy. This slope is also consistent with the bandgap narrowing measured on the same samples by photomodulated reflectance and is consistent with the band anticrossing model for the splitting of the conduction band in the GaN_xAs_{1-x} alloys. Lithographically patterned GaN_xAs_{1-x} dots are imaged by BEEM. Analysis of BEEM spectra of the locally confined dots indicates an alloying-induced decrease in the Schottky barrier height of four times the thermal energy at room temperature. © *2008 American Institute of Physics*. [DOI: 10.1063/1.3041154]

I. INTRODUCTION

Highly mismatched semiconductor alloys (HMAs) have become important due to their dramatic changes in electronic properties from the host materials, which suggests many potential technological applications.[1] GaN_xAs_{1-x} is a HMA known especially for its large bandgap reduction, or bowing of as much as 180 meV per $x=0.01$ up to a few percent N.[2] Although thin films of this material have been fabricated and studied, the composition of two dimensionally (2D) patterned devices must be controlled not only in the growth direction but also in the lateral directions. The synthesis of quantum dots and wires has been largely based on spontaneous growth processes using the lattice mismatch and wetting behavior between substrates and the depositing materials.[3] Ion implantation (II) of N into GaAs followed by a combination of pulsed-laser melting (PLM) and rapid thermal annealing (RTA) has recently been shown to produce high-quality thin films of GaN_xAs_{1-x}.[4,5] The extremely fast melting and solidification rate in the PLM process (<100 ns) results in highly supersaturated, substitutional solid solutions[6] giving rise to a large bandgap reduction comparable to that found in alloys produced by conventional thin film growth methods. Hence, patterned II followed by unpatterned transient thermal processing might permit lateral control of the conduction band edge, thereby enabling the development of a variety of 2D quantum devices from HMAs.

In ballistic electron emission microscopy (BEEM), a three-terminal scanning tunneling microscope (STM) is used to measure the electronic band structure of a buried semiconductor heterostructure by collecting carriers filtered by the Schottky barrier at a metal-semiconductor interface.[7] BEEM has been used to image self-assembled quantum dots embedded in III-V semiconductors and observe the resonant behaviors with nanometer scale spatial resolution.[8] The BEEM technique has also been applied to the investigation of GaN_xAs_{1-x} thin films grown by low-temperature molecular beam epitaxy (LT-MBE) and reveals that the Schottky barrier height decreases with increasing nitrogen concentration.[9] In a previous study,[10] we used BEEM and spectrometry to characterize 2D patterned GaN_xAs_{1-x} nanostructures fabricated by patterned nitrogen II followed by PLM and RTA. Here, we systemically investigate the effects of the incorporated nitrogen concentrations on the band structure of the GaN_xAs_{1-x} alloy synthesized by II-PLM-RTA, through a combination of BEEM and photomodulated reflectance (PR) spectroscopy made on the same samples.

II. EXPERIMENT

A 200 nm undoped GaAs layer was epitaxially grown on a (001)-oriented n^+ GaAs substrate. 2D patterning of quantum structures was achieved with the aid of a polymethylmethacrylate (PMMA) mask created by electron-beam lithography was used. The 400 nm thick mask had an array of holes of 75 nm diameter and 1.2 μm period over a 600

a)Electronic mail: kim57@fas.harvard.edu.

 © 2008 American Institute of Physics

Downloaded 11 Dec 2008 to 140.247.59.237. Redistribution subject to AIP license or copyright; see http://jap.aip.org/jap/copyright.jsp

$\times 600\ \mu m^2$ area. Nitrogen ions (N^+) were implanted into the mask, which is designed to be thick enough to block all the implanted ions except those traversing the holes. By using an ion energy of 20 keV with varied doses from 0.9×10^{15} to $4.6\times10^{15}/cm^2$, the selectively exposed GaAs regions were implanted to a depth of approximately 100 nm with nitrogen atomic concentration ranging from 1.3×10^{20} to $6.8\times10^{20}/cm^3$ at the peak of the distribution. For comparison, some samples were implanted without the mask under identical implantation conditions and will be referred as planar-processed samples.

After removal of the PMMA mask by oxygen plasma ashing,[11] the GaAs samples were pulsed-laser melted in air using a XeCl excimer laser ($\lambda=308$ nm) with a pulse duration ~30 ns full width at half maximum. The laser beam was formed into a uniform rectangular shape spot with less than 4% rms intensity variation with a multiprism beam homogenizer. The melt durations (τ_{melt}) were determined by measuring the time resolved reflectivity of the samples using a low-power continuous-wave argon-ion (488 nm) probe laser. The excimer laser fluence reported in this paper was estimated by the melt duration versus fluence relationship that comes from a numerical solution of the one-dimensional (1D) heat equation.[12] The measured melt duration of pure, unimplanted GaAs (001) ranged from 48 to 76 ns for fluences identified through heat-flow simulation to range from 0.27 to 0.33 J/cm^2, respectively. This procedure provides a fluence calibration with an estimated uncertainty of $\pm0.01\ J/cm^2$. This range of fluence was observed to cause the measured melt duration on the implanted, planar-processed sample ranging from 55 to 99 ns. Some of the samples were treated by RTA after PLM at temperatures between 850 and 950 °C for 5–10 s in flowing N_2 as reported in a previous study.[4] The structure of the planar-processed GaN_xAs_{1-x} samples was studied by channeling Rutherford backscattering spectrometry (c-RBS). 2 MeV He^+ ions were used for c-RBS and channeling was performed in the ⟨001⟩ direction. The nitrogen concentration in some samples was determined by secondary ion mass spectrometry (SIMS) performed on a Physical Electronics 6650 quadruple mass spectrometer using a 6 keV Cs^+ primary beam at an incident angle of 60° from the surface normal and monitoring the $^{75}As^-$ and $^{83}GaN^-$ secondary ions.

Samples for BEEM were prepared by depositing Cr/Au Ohmic contacts on the underside of the n^+ GaAs substrates, and Schottky contacts, consisting of Au layers (8 nm thick), were deposited on the samples by thermal evaporation at a typical background pressure of 3×10^{-7} torr. Prior to Au evaporation, the pulsed-laser-melted GaAs surfaces were treated in a 1:10 solution of $NH_4OH:H_2O$ for 60 s followed by ~3 s rinse in de-ionized water. The Au contacts were 0.9 mm in diameter and made by photolithography.[13] The BEEM measurements were performed in air at room temperature with a surface/interface AIVTB-4 BEEM/STM system using a Au tip.

The optical transitions characterizing the bandgaps of the planar-processed alloys were measured by room temperature PR. Radiation from a 300 W halogen tungsten lamp dispersed by a 0.5 m monochromator was focused on the sample as a probe beam. A chopped (311 Hz) HeCd laser beam (325 nm) provided the photomodulation. PR signals were detected by a Si or Ge photodiode using a phase sensitive lock-in amplification system. The bandgap and broadening were determined by fitting the PR spectra to the Aspnes third-derivative functional form,[14]

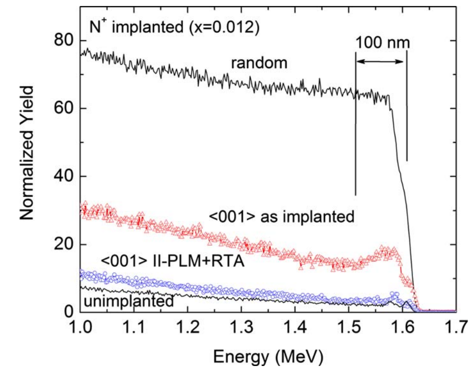

FIG. 1. (Color online) (Open triangles) c-RBS measured in the ⟨001⟩ axial direction from N^+-implanted GaAs samples as implanted ($3.76\times10^{15}/cm^2$ at 20 keV) and (open circles) after laser melting using 0.31 J/cm^2 (90 ns) followed by RTA at 950 °C for 10 s in 1 atm of N_2. For comparison, the channeled and the random spectra from an unimplanted GaAs (001) substrate are shown by solid lines.

$$\frac{\Delta R}{R}=\mathrm{Re}(Ce^{i\theta}\Delta\varepsilon), \quad (1)$$

where $\Delta\varepsilon$, the field-induced change in the dielectric function, has the resonant form $\Delta\varepsilon\sim(E_g-\hbar\omega-i\Gamma)^{-n}$, and E_g is the bandgap energy, Γ is the broadening, C is the amplitude, and θ is the phase to determine the line shape.

III. RESULTS AND DISCUSSION

Figure 1 shows the recovery of crystalline structure after PLM and RTA processes measured by c-RBS in the ⟨001⟩ axial direction. The channeled spectrum from the as-implanted sample reveals a high amount of dechanneling from the top 100 nm, showing the presence of amorphous or heavily damaged crystalline material. c-RBS after the laser melting and RTA processes shows a minimum backscattered yield χ_{min} of 5.7% of that from a random direction, which indicates that these samples are almost indistinguishable by ion channeling from the unimplanted GaAs (001) substrate whose χ_{min} is 4.1%.

The SIMS nitrogen depth profiles in Fig. 2 show that nitrogen redistribution has occurred following PLM and RTA. The simulated profiles were determined through numerical simulation of the 1D linear diffusion equation, using as input the measured as-implanted nitrogen depth profile and the melt depth versus time that comes from a numerical solution of the 1D heat equation.[12] The diffusivity in the melt is assumed to be $D_N^{l\text{-GaAs}}=0.9\times10^{-4}\ cm^2/s$, while that in the solid is assumed to be zero. During solidification, the nitrogen partition coefficient k at the moving crystal-melt interface is assumed to be a constant value of 0.13 or 0.51 for the higher (0.33 J/cm^2) and lower (0.27 J/cm^2) fluence laser irradiations, respectively. The heat-flow simulation results indicate that the solidifying velocity of the solid/liquid inter-

Downloaded 11 Dec 2008 to 140.247.59.237. Redistribution subject to AIP license or copyright; see http://jap.aip.org/jap/copyright.jsp

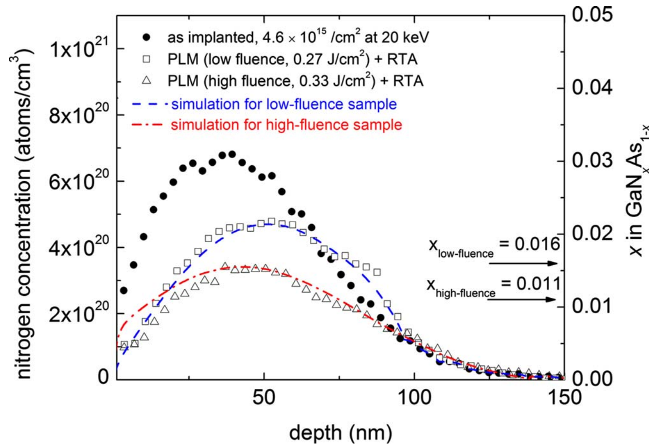

FIG. 2. (Color online) SIMS depth profile of nitrogen concentration for as-implanted ($4.64\times10^{15}/\mathrm{cm}^2$ at 20 keV, solid circles) and PLM+RTA samples. The PLM was performed at 0.27 (open squares, "low fluence") and 0.33 $\mathrm{J/cm^2}$ (open triangles, "high fluence"), resulting in melt durations of 65 and 99 ns, respectively. Both laser melted samples were treated by RTA at 950 °C for 5 s in 1 atm of N_2. 1D diffusion simulated profiles are shown as dashed and dashed dotted lines with best-fit parameters given in Table I. The arrows indicate the values of x assigned to the PLM+RTA samples, which are the averaged concentrations within the calculated melt depths given in Table I.

face over the depth range of significant interaction with the nitrogen profile has average values of 2.9 and 3.1 m/s, with ranges of 2.5–3.5 and 2.6–3.5 m/s, for the higher and lower laser fluences, respectively. These results suggest a velocity-dependent partition coefficient[6] with a significantly higher sensitivity of partition coefficient to velocity than in any previously explored behavior in silicon.[15] These results, however, are considerably less reliable than those in previous studies because here the solidification velocity was not measured directly and the thermophysical parameters of GaAs are not as well known as those of silicon. At the free surface, nitrogen evaporation from the melt was assumed to occur with an evaporative flux given by $v_{\mathrm{evap}}C_0^m$, where C_0 is the (time-dependent) nitrogen concentration at the surface, m is the order of the reaction, and v_{evap} is the surface recombination velocity for evaporation. Here v_{evap} is equal to 2.56 m/s, which implies a surface lifetime in the topmost (004) monolayer of 0.055 ns. Evaporation might take place by either a unimolecular ($m=1$) or a bimolecular ($m=2$) process. Because the simulated profiles for the two cases were indistinguishable, we show the results for unimolecular evaporation. The RTA process itself has been shown to cause no observable redistribution[16] of the implanted nitrogen profile in GaAs, and thus the nitrogen evaporation from our samples is modeled as occurring only during the laser melting process, despite the sub-100 ns melt duration. The diffusion simulation parameters used in this article are summarized in Table I. Uncertainties reported for simulation parameters are estimates based on a qualitative judgment of the onset of significant deviation of the simulated and measured final nitrogen depth profiles.

In Fig. 3(a), we compare the second derivative (SD) BEEM spectra of the planar-processed GaN_xAs_{1-x} implanted without a mask at 20 keV and four different doses, followed by 0.30 $\mathrm{J/cm^2}$ of PLM and RTA at 950 °C for 5 s. The

TABLE I. 1D diffusion simulation parameters for fitting final nitrogen-concentration depth profiles for low (0.27 $\mathrm{J/cm^2}$) and high (0.33 $\mathrm{J/cm^2}$) fluence samples.

Laser fluence, experimental ($\mathrm{J/cm^2}$)	0.27 ± 0.01	0.33 ± 0.01
Laser fluence ($\mathrm{J/cm^2}$) used in simulation	0.26 ± 0.01	0.32 ± 0.01
Maximum melt depth (nm) in simulation	100 ± 3	140 ± 7
k	0.51 ± 0.1	0.13 ± 0.02
$D_{\mathrm{N}}^{l\text{-GaAs}}$ ($\mathrm{cm^2/s}$)	0.9 ± 0.1	0.9 ± 0.1
v_{evap} (m/s)	2.56 ± 1.0	2.56 ± 1.0

BEEM spectra were obtained with a constant tunneling current (I_t) of 2 nA and a varying tip bias (V_t) that ranged from 0.4 to 2.2 V. The room temperature SD-BEEM spectra extracted from the measured BEEM spectra are approximately the heterostructure transmission coefficients of the collector current, such that features in the spectra can be used to identify specific hot electron transport channels.[17] The dotted line

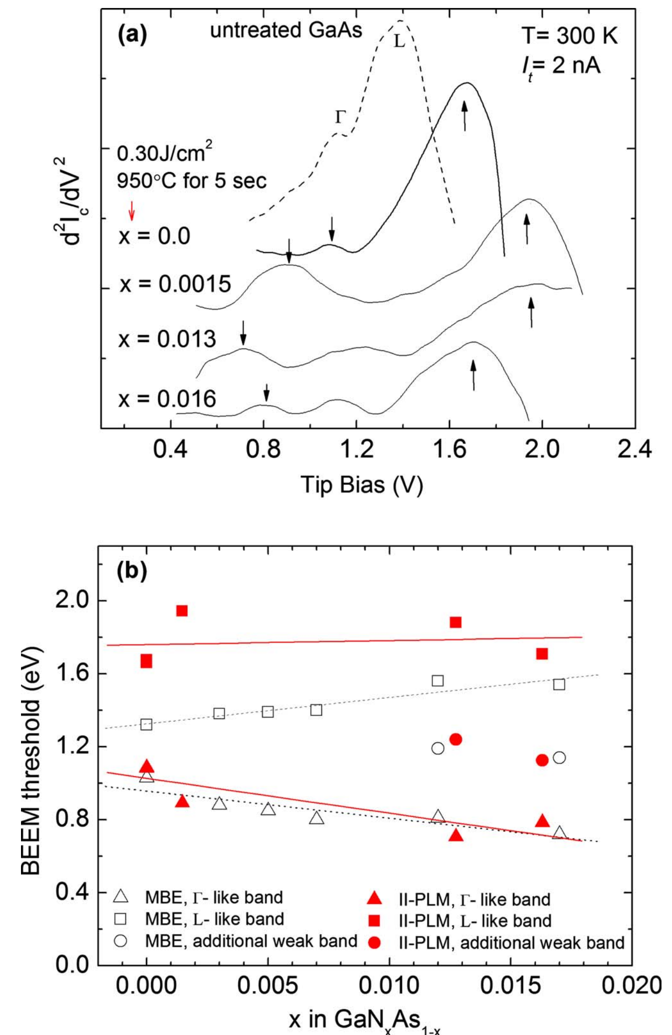

FIG. 3. (Color online) (a) SD-BEEM spectra for different nitrogen concentrations. The spectra are vertically offset arbitrarily for clarity. The topmost dotted line represents the SD spectrum of the unprocessed GaAs substrate without implantation. (b) Composition dependence of thresholds observed at the peaks of the SD-BEEM spectra of GaN_xAs_{1-x}. The open symbols are the thresholds for LT-MBE grown GaN_xAs_{1-x} (Ref. 9), and the solid symbols are for the thresholds for II-PLM-RTA GaN_xAs_{1-x} measured in this work. The lines are linear fits of the concentration dependence for MBE grown (dotted) and II-PLM (solid) samples.

Downloaded 11 Dec 2008 to 140.247.59.237. Redistribution subject to AIP license or copyright; see http://jap.aip.org/jap/copyright.jsp

represents the SD spectra of an unprocessed GaAs substrate without implantation, laser melting, or RTA; the two main peaks can be identified as the Γ and L peaks of GaAs as described in our previous work.[9] These peaks, indicated by arrows, appear to split apart with increasing nitrogen composition[18] (x) in the II-PLM samples before the trend is reversed at the highest nitrogen composition. In Fig. 3(b), we compare the energies of those peaks (thresholds) of II-PLM samples with the corresponding measurements for LT-MBE grown GaN_xAs_{1-x},[9] as a function of nitrogen concentration. The lines are linear fits for the concentration dependence of the thresholds in MBE grown (dotted) and II-PLM (solid) samples. The Γ-like thresholds (Schottky barriers for Au/GaN_xAs_{1-x}) decrease as the nitrogen concentration increases for both fabrication methods. The linear fit to the Γ-like peaks for the II-PLM samples gives a slope of -191 ± 63 meV per $x=0.01$, which is close to the corresponding slope (-164 meV per $x=0.01$) for the LT-MBE grown samples. The extra peaks, which show up for higher concentration ($x>0.012$), might be due to additional weak bands as observed in LT-MBE grown GaN_xAs_{1-x}. Furthermore, the deviation from the linear fit for Γ-like thresholds of II-PLM samples may be due to the increased surface scattering for the laser melted samples.

The PR spectra exhibit features related to the fundamental bandgap transitions from the samples measured by BEEM as shown in Fig. 4(a). The sharp transitions present in each spectrum at 1.43 eV arise from the transitions from the unimplanted region of the GaAs substrate due to its strong absorption of the HeCd probe laser. The bandgaps between the valence band maximum and the lower conduction subband E_- of the synthesized GaN_xAs_{1-x} layer are observed at energies lower than the fundamental of GaAs measured for the unimplanted sample as indicated by the arrows. In Fig. 4(b), the fitted bandgap energies for the GaN_xAs_{1-x} layer are plotted versus nitrogen concentration. The dashed line represents the E_- conduction subband in the band anticrossing (BAC) model,[19,20] which is given by

$$E_{\pm}(k)=\frac{1}{2}\{E_{\mathrm{N}}+E_M(k)\pm\sqrt{[E_{\mathrm{N}}-E_M(k)]^2+4C_{\mathrm{NM}}^2x}\},\quad (2)$$

where E_{N} is the energy of the N level, $E_M(k)$ is the dispersion relation for the host matrix, and the C_{NM} is the matrix element for the coupling between N states and the extended states. Here, we used the GaN_xAs_{1-x} parameter values of $E_{\mathrm{N}}=1.65$ eV, $E_M=1.43$ eV, and $C_{\mathrm{NM}}=2.7$ eV as established previously to fit the experimental data.[20] We compare our results with the bandgaps from Yu *et al.*[5] In both studies, the decrease in bandgap with increasing implanted nitrogen concentration is observed. Because our identification of the nitrogen concentration for the abscissa was done by averaging the SIMS profile over the maximum melt depth instead of reporting the peak concentration as in Ref. 5, the N concentration, x, corresponding to the PR transitions in our GaN_xAs_{1-x} layers may be underestimated.

The Au/GaN_xAs_{1-x} Schottky barrier heights, or the Γ-like thresholds from the II-PLM samples, show a decrease with increasing x comparable to that of the bandgap energies measured by the PR on the same samples. To compare them directly, in Fig. 5 we shifted the Γ-like thresholds vertically

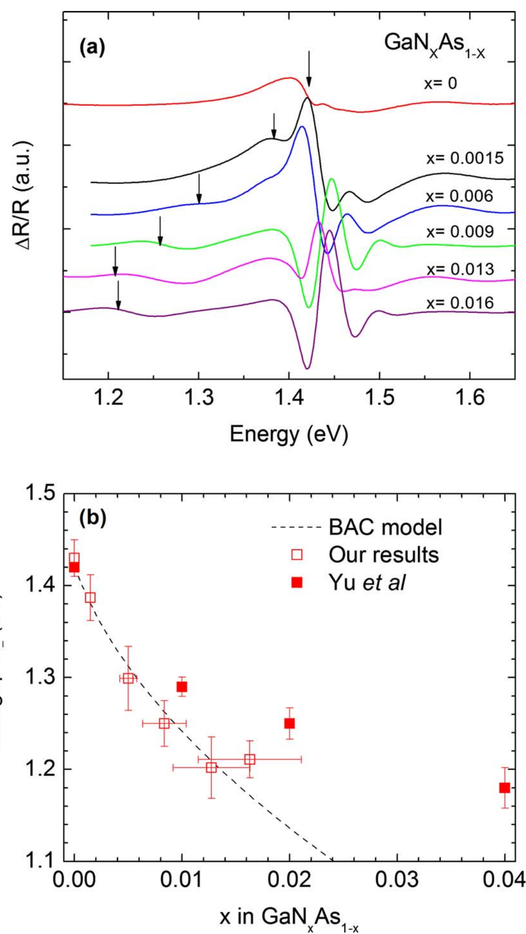

FIG. 4. (Color online) (a) A series of room temperature PR spectra measured for the N^+-implanted GaAs after PLM ($0.30\ J/cm^2$) and RTA at 950 °C for 5 s in 1 atm of N_2. The arrows indicate the position of the lowered subband (E_-) by fitting. The bandgap energies from the fitting of PR spectra are plotted vs nitrogen concentration in (b). The dashed line is the calculated bandgap energies based on the BAC model.

by the difference between the BEEM measured threshold (0.93 eV) and the PR measured bandgap energy (1.43 eV) from an unimplanted GaAs specimen. This comparison implies that the nitrogen induced Schottky barrier reduction in our II-PLM samples is mostly from the bandgap reduction in GaN_xAs_{1-x}, as in the MBE grown samples (open triangles),

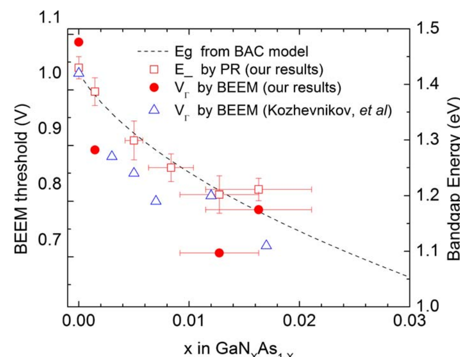

FIG. 5. (Color online) Comparison of bandgap energies from PR measurement and the Schottky barrier heights from BEEM measurement. The spectra are vertically offset arbitrarily for clarity. The dashed line is the calculated bandgap energy based on the BAC model.

Downloaded 11 Dec 2008 to 140.247.59.237. Redistribution subject to AIP license or copyright; see http://jap.aip.org/jap/copyright.jsp

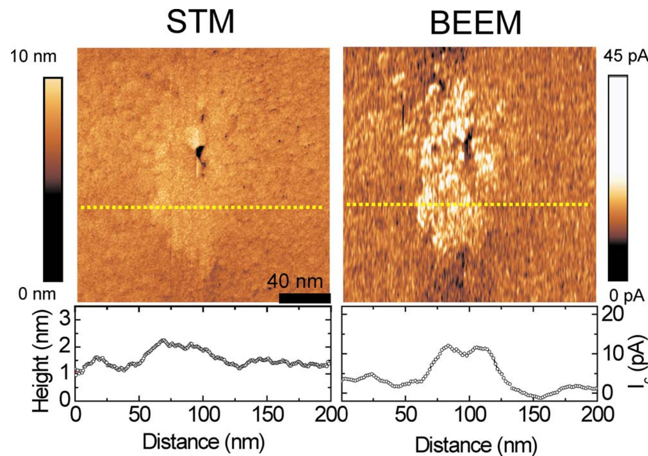

FIG. 6. (Color online) STM and BEEM images of one of the implanted GaN_xAs_{1-x} dots. Both images are measured simultaneously at $V_t=-1.0$ V and $I_t=2$ nA. The Au grains and N^+-implanted dot (~120 nm diameter in the center) are visible in the STM image, and an enhancement of the BEEM current is observed at the implanted region. The sample was implanted with $1.77\times10^{15}/cm^2$ of N^+ at 20 keV, followed by 0.31 J/cm^2 of PLM and RTA at 950 °C for 10 s. The section profile below each image was measured along the dashed lines and smoothed to show the trend more clearly.

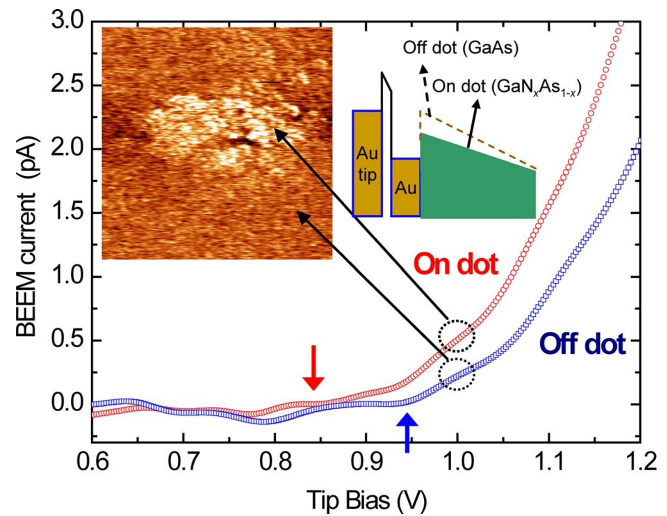

FIG. 7. (Color online) BEEM spectra on and off the synthesized dot imaged in Fig. 6, exhibiting shift in thresholds on the dot at tip bias below the Schottky barrier height of unimplanted surrounding GaAs. The arrows indicate best-fit BEEM thresholds for on dot (0.84 V) and off dot (0.93 V). The sample was implanted with $1.77\times10^{15}/cm^2$ of N^+ at 20 keV, followed by 0.31 J/cm^2 of PLM and RTA at 950 °C for 10 s.

and the effects of nitrogen incorporation on the valence band are small compared to those on the conduction band, which agrees well with other studies.[9,16,21]

Figure 6 shows the STM and BEEM images of a dot made by patterned N^+ implantation followed by PLM and RTA. The dot was implanted with $1.77\times10^{15}/cm^2$ of N^+ at 20 keV, corresponding to $x\sim0.005$ estimated from the SIMS measurement on the planar-processed samples as shown in Fig. 2. In the STM image, the Au grains (~10 nm) and the N^+-implanted region are visible. The original implanted dot diameter of 80 nm has grown to about 120 nm, which is likely due to the lateral diffusion of nitrogen during pulsed-laser melting. The BEEM image was obtained from a tunneling current of 2 nA and a tip voltage was fixed at −1.0 V, which is above the Schottky barrier height for the Au/GaAs interface. A strong enhancement (~10 pA) of the BEEM current is observed within the patterned region.

To confirm the source of this higher BEEM current on the dot region, BEEM spectra were taken on and off the dot. Figure 7 shows the BEEM spectra averaged over 200 voltage scans for each region in order to increase the signal to noise ratio. The thresholds were inferred from a two valley Bell–Kaiser (BK) (Ref. 22) least-squares fit, which is expressed as

$$I_c(V) = R_{\Gamma,L}I_t\frac{\int_{E_{z\,\min}}^{\infty} D(E_z,V)\int_0^{E_{t\,\max}} F(E)dE_t dE_z}{\int_0^{\infty} D(E_z,V)\int_0^{\infty}[F(E)-F(E+eV)]dE_t dE_z}, \tag{3}$$

where V is the tip bias, I_t is the tunneling current, D is the WKB tunneling probability, and F is the Fermi function. The integration limits are determined by transverse momentum conservation and set to $E_{z\,\min}=E_F-e(V-V_{b\Gamma,bL})$ and $E_{t\,\max}=m_t/(m-m_t)\{E_z-E_F+e(V-V_{b\Gamma,bL})\}$. E_F is the Fermi energy in the Au tip, and $m_t(m)$ is the transverse effective mass in the semiconductor (metal). $R_{\Gamma,L}$ and $V_{b\Gamma,bL}$ are attenuating factors and the Schottky barriers related to the Γ or L valley transition, respectively, and used as adjustable parameters during fitting.[13,22] The fitting results exhibit a shift of the initial Γ threshold from 0.93 to 0.84 V when the tip moves from the surrounding GaAs to the patterned dot area, as indicated by the arrows. The small structures in the off-dot spectrum below the main threshold of 0.93 V represent fluctuation in the signal to noise ratio. Significant BEEM current is measurable only above about 0.9 V for the off-dot spectrum, which was used as a starting point for the BK fitting. The kink at around 0.9 V of the on-dot spectrum might be real and related to the buried undoped GaAs left between the nitrogen implanted depth (~100 nm) and the n^+ GaAs substrate. The nitrogen implanted sample, however, shows measurable BEEM current at lower threshold Schottky barrier and the simple BK fitting was intended to simply get the lowest thresholds in this study. This threshold reduction, which is at least four times the room temperature thermal energy of electrons, opens the possibilities of producing an arbitrarily patterned quantum confined structure using II-PLM-RTA, and of imaging the structure with BEEM.

IV. CONCLUSIONS

In this work, single crystalline GaN_xAs_{1-x} alloys using II-PLM-RTA were created. The redistribution of nitrogen during PLM is consistent with nitrogen diffusion in the liquid phase characterized by a diffusivity of $D_N^{l\text{-GaAs}}=0.9\times10^{-4}$ cm^2/s, evaporation from the surface characterized by a surface recombination velocity of 2.56 m/s, and solute trapping at the rapidly moving solidification front characterized by a nonequilibrium partition coefficient in excess of 0.1. The dependence of the partition coefficient on solidification speed appears to be steeper than in any previous report, but experimental uncertainties preclude a definitive conclusion.

Downloaded 11 Dec 2008 to 140.247.59.237. Redistribution subject to AIP license or copyright; see http://jap.aip.org/jap/copyright.jsp

BEEM spectra taken on planar-processed GaN_xAs_{1-x} alloys synthesized by II-PLM-RTA indicate for the lowest conduction band (the Γ-like valley) a Schottky barrier height reduction with increasing nitrogen content of -191 ± 63 meV per $x=0.01$, which is close to the corresponding slope (-164 meV per $x=0.01$) for LT-MBE grown samples. The higher conduction band at the *L*-like valley exhibits a threshold that is imperceptibly sensitive to composition, in contrast to the slight increase with composition exhibited by the LT-MBE grown materials. In both types of materials, an unidentified intermediate band appears for $x>0.012$.

PR measurements on the same samples reveal optical transitions characterized by a bandgap that decreases with increasing nitrogen content at the same rate of decrease as that of the Γ-like valley as indicated by the Schottky barrier height in the BEEM measurement. These results are consistent with the BAC model of Walukiewicz *et al.*[19,20] for the splitting of the conduction band, which is known to explain the *x*-dependence of the bandgap narrowing.

By analyzing the BEEM spectra of lithographically fabricated locally confined dots, we observed the decrease in the Schottky barrier height with nitrogen incorporation within the dot that is four times the thermal energy at room temperature. This result bodes well for the possibility of fabricating arbitrarily patterned 2D nanostructures of GaN_xAs_{1-x} in GaAs with lateral electron confinement.

ACKNOWLEDGMENTS

We thank Dr. Jeffrey M. Warrender for valuable discussions and technical assistance with simulating surface evaporation. We also thank Professor Russell D. Dupuis and Professor Arthur Gossard for providing epitaxial substrates. This work was supported by a DARPA HUNT Contract No. 222891-01 subaward from the University of Illinois at Urbana-Champaign, and by the National Science Foundation under Grant No. NSF-ECCS-0701417. The support of the Center for Nanoscale Systems (CNS) at Harvard University is also acknowledged. Harvard-CNS is a member of the National Nanotechnology Infrastructure Network (NNIN), which is supported by the National Science Foundation under NSF Award No. ECS-0335765. PR measurements and rapid thermal processing of samples were supported by the Director, Office of Science, Office of Basic Energy Sciences, Division of Materials Sciences and Engineering, of the U.S. Department of Energy under Contract No. DE-AC02-05CH11231. K.A. acknowledges support from a NSF-IGERT fellowship.

[1] J. W. Ager and W. Walukiewicz, Semicond. Sci. Technol. **17**, 741 (2002).
[2] K. Uesugi, N. Morooka, and I. Suemune, Appl. Phys. Lett. **74**, 1254 (1999); M. Kondow, K. Uomi, K. Hosomi, and T. Mozume, Jpn. J. Appl. Phys., Part 2 **33**, L1056 (1994).
[3] P. M. Petroff, A. Lorke, and A. Imamoglu, Phys. Today **54**(7), 46 (2001); Q. Xie, A. Madhukar, P. Chen, and N. P. Kobayashi, Phys. Rev. Lett. **75**, 2542 (1995).
[4] K. M. Yu, W. Walukiewicz, J. W. Beeman, M. A. Scarpulla, O. D. Dubon, M. R. Pillai, and M. J. Aziz, Appl. Phys. Lett. **80**, 3958 (2002).
[5] K. M. Yu, W. Walukiewicz, M. A. Scarpulla, O. D. Dubon, J. Wu, J. Jasinski, Z. Liliental-Weber, J. W. Beeman, M. R. Pillai, and M. J. Aziz, J. Appl. Phys. **94**, 1043 (2003).
[6] M. J. Aziz, Metall. Mater. Trans. A **27**, 671 (1996).
[7] V. Narayanamurti and M. Kozhevnikov, Phys. Rep. **349**, 447 (2001).
[8] M. E. Rubin, G. Medeiros-Ribeiro, J. J. O'Shea, M. A. Chin, E. Y. Lee, P. M. Petroff, and V. Narayanamurti, Phys. Rev. Lett. **77**, 5268 (1996); M. E. Rubin, H. R. Blank, M. A. Chin, H. Kroemer, and V. Narayanamurti, Appl. Phys. Lett. **70**, 1590 (1997).
[9] M. Kozhevnikov, V. Narayanamurti, C. V. Reddy, H. P. Xin, C. W. Tu, A. Mascarenhas, and Y. Zhang, Phys. Rev. B **61**, R7861 (2000).
[10] T. Kim, M. J. Aziz, and V. Narayanamurti, Appl. Phys. Lett. **93**, 102117 (2008).
[11] J. I. McOmber, K. Ostrowski, M. Meloni, R. Eddy, and P. Buccos, Nucl. Instrum. Methods Phys. Res. B **74**, 266 (1993).
[12] D. E. Hoglund, M. O. Thompson, and M. J. Aziz, Phys. Rev. B **58**, 189 (1998).
[13] J. J. O'Shea, E. G. Brazel, M. E. Rubin, S. Bhargava, M. A. Chin, and V. Narayanamurti, Phys. Rev. B **56**, 2026 (1997).
[14] D. E. Aspnes, Surf. Sci. **37**, 418 (1973).
[15] J. A. Kittl, P. G. Sanders, M. J. Aziz, D. P. Brunco, and M. O. Thompson, Acta Mater. **48**, 4797 (2000).
[16] W. Shan, K. M. Yu, W. Walukiewicz, J. W. Ager, E. E. Haller, and M. C. Ridgway, Appl. Phys. Lett. **75**, 1410 (1999).
[17] D. L. Smith and S. M. Kogan, Phys. Rev. B **54**, 10354 (1996).
[18] The value of *x* reported for all as-implanted profiles is the peak of the nitrogen-concentration depth distribution, and the value of *x* and its error bar reported for all PLM and PLM+RTA specimens is the averaged concentration and the standard deviation within the calculated melt depth.
[19] W. Shan, W. Walukiewicz, J. W. Ager III, E. E. Haller, J. F. Geisz, D. J. Friedman, J. M. Olson, and S. R. Kurtz, Phys. Rev. Lett. **82**, 1221 (1999).
[20] J. Wu, W. Shan, and W. Walukiewicz, Semicond. Sci. Technol. **17**, 860 (2002).
[21] W. Shan, W. Walukiewicz, J. W. Ager, E. E. Haller, J. F. Geisz, D. J. Friedman, J. M. Olson, and S. R. Kurtz, J. Appl. Phys. **86**, 2349 (1999).
[22] L. D. Bell and W. J. Kaiser, Phys. Rev. Lett. **61**, 2368 (1988).

Downloaded 11 Dec 2008 to 140.247.59.237. Redistribution subject to AIP license or copyright; see http://jap.aip.org/jap/copyright.jsp